

## INFLUENCE OF IMPURITIES AND ION SURFACE ALLOYING ON THE CORROSION RESISTANCE OF E110 ALLOY

<sup>1</sup>Kalin B.A., <sup>1</sup>Volkov N.V., <sup>1</sup>Valikov R.A., <sup>2</sup>Novikov V.V., <sup>2</sup>Markelov V.A., <sup>3</sup>Pimenov Yu.V.

<sup>1</sup> National Research Nuclear University «MEPhI» (NRNU MEPhI),

<sup>2</sup> JSC the Federal State Unitary Enterprise, A.A. Bochvar All-Russia Research Institute of Inorganic Materials (JSC «VNIINM»),

<sup>3</sup> JSC TVEL Corporation (JSC «TVEL»)

### Introduction

The corrosion resistance of zirconium alloys depends on their structural-phase state, the type of core coolant and operating factors. The formation of a protective oxide film on the zirconium alloys is sensitive to the content of impurity atoms present in the charge base of alloys and accumulating in them in the manufacture of products. The impurity composition of the initial zirconium is determined by the method of its manufacture and generally remains unchanged in the products, determining their properties, including their corrosion resistance. An increased content of impurities (C, N, Al, Mo, Fe) both individually and in their combination negatively affects the corrosion resistance of zirconium and its alloys [1].

One of the potentially effective methods to increase the protective properties of oxide films on zirconium alloys is a surface alloying using the regime of mixing the atoms of a film, preliminarily coated on the surface, and the atoms of a target [2-6]. This method makes it possible to form a given structural-phase state in the thin surface layer with unique physicochemical properties and thus to increase the corrosion resistance and wear resistance of fuel claddings [2-3].

In this context, the object of investigation was samples of cladding tubes from alloy E110 with various content of impurity elements (nitrogen, aluminum, and carbon) with the aim to reduce the negative influence of impurities on the corrosion resistance by changing the structural-phase state of the surface layer of fuel claddings and fuel assembly components with alloying in the regime of ion mixing of atoms.

### Experimental technique

*Material and sample preparation technique.* Fuel claddings with a diameter of 9.1-9.5 mm and a wall thickness of 0.6 mm made from alloy E110 and its various smeltings based on zirconium sponge: 5001, 5002, 5005, 5008, 5027 and 301, were chosen as a material for investigation. The composition of the analyzed impurities of the smeltings is shown in Table 1. It is seen from the table that the concentration of carbon atoms varied from 79 ppm (smelting 5005) to 140 ppm (smelting 5001), nitrogen – from 35 ppm (smelting 5005) to 100 ppm (smelting 301), aluminum – from 10 ppm (smelting 301) to 80 ppm (smelting 5008).

Samples for alloying the surface layer in the regime of ion mixing were cut from tubes in the form of segments 10 mm in length (fig. 1) and subjected to chemical etching and polishing in an electrolyte  $\text{CH}_3\text{COOH} + 10\% \text{HClO}_4$  (the electrolyte temperature was  $0^\circ\text{C}$ , the voltage on the electrodes was equal to 30 V, and the current was 0.15 A), and a part of the samples was subjected to surface cleaning by an argon ion beam with a wide energy spectrum, the parameters of which are specified below.

Alloying of the outer sample surface was carried out by ion mixing (implantation of atoms from a film) under irradiation by a beam of  $\text{Ar}^+$  ions [3]. For this purpose before the irradiation, films of the following elements: C, Al, Fe, Mo and Mo-Fe-Al, with a thickness  $x_i=30 - 50$  nm of each element were sputtered onto the surface of samples by thermal evaporation in vacuum ( $P = 3 \times 10^{-4}$  Pa) (fig. 1). Then the samples were irradiated at the installation VOCAL by a beam of  $\text{Ar}^+$  ions with a wide energy spectrum from 1 to 17 keV, at a mean ion energy in the beam  $\langle E \rangle = 10$  keV, at the current of the ion beam varying in the 10 – 50  $\mu\text{A}$  range, at the ion beam section of  $15 \times 15$  mm, at the pressure of residual gases in the working chamber  $P < 1 \times 10^{-5}$  Pa, at the irradiation temperature of 50 – 150  $^\circ\text{C}$ , and at an irradiation dose of  $\Phi = (1 - 100) \times 10^{17} \text{ cm}^{-2}$  [5].

The use of ion beams with a wide energy spectrum allows carrying out an ion treatment of targets with a minimum level of radiation damages and getting a sufficiently uniform distribution of the implanted atoms in the target surface layer [1-3].

*Research methods of oxide films.* The surface state of samples was visually examined in a scanning electron microscope microanalyzer (SEM) EVO-50 and the structure of oxide films along their thickness on alloys was investigated using scanning ion microscopes (SIM) Strata-235 and Quanta-500 with a probe beam of  $\text{Ga}^+$  ions under the following parameters: the ion energy – 30 keV, the ion beam current – 1-10 nA, the beam cross-section – 10-30 nm, the residual gas pressure in the working chamber was better than  $10^{-8}$  Pa, as well as the microanalyzer of a scanning electron microscope JSM-840 (Company "Jeol") with an X-ray microprobe analyzer ISIS (Company "Oxford Instruments") integrated with it, a secondary ion mass spectroscopy – SIMS (device HPI-660, Company HPI, USA) and an XRF analysis (spectrometer Orbis PC Micro-XRF, Company EDAX) were used. To estimate the thickness of oxide films, ion microscopy was used together with infrared scanning microscopy. The surface roughness of samples was determined using a profilometer- profilograph TR-200 (Company A&D) according to GOST 2789-73.

*Corrosion tests of samples.* The corrosion tests of samples were carried out using the technique of ASTM ISO № 10270 "Corrosion of metals and alloys in aqueous media" in autoclaves, made of austenitic stainless steel, in water at the temperature of  $360^\circ\text{C}$  ( $P = 18.6$  MPa) with removing of oxygen. The tests were conducted for 300, 720, 2160, 3600 and 4240 h.

## Experimental results

The surface roughness of metal samples subjected to chemical polishing and cleaning by sputtering the target atoms by a beam of argon ions (chemical polishing (Chem-Pol) + Ar<sup>+</sup>) as well as oxidation was studied during their preparation for corrosion tests and after these tests. The samples roughness parameter before the oxidation was equal to  $R_a = 0.20 \pm 0.07 \mu\text{m}$  and did not depend on the alloy composition. After the oxidation for 300 h, the roughness parameter  $R_a$  was practically increased and, for example, for smelting 5001-08 it was  $R_a = 0.37 \pm 0.07 \mu\text{m}$ .

The results on corrosion tests of the samples of alloys in the initial state (the state of tubes delivery – column 9) are shown in Table 2, as well as of the samples after the treatment in three states (column 3): I – mechanical polishing + ion cleaning under irradiation by Ar<sup>+</sup> ions, II – chemical polishing + irradiation by Ar<sup>+</sup> ions, III – chemical polishing + ion alloying by carbon atoms that are presented in the form of overweights and thicknesses of oxide films (column 4), including those determined on an ion scanning microscope (column 5) and on an infrared spectrometer from the outer (column 6) and internal (column 7) tube surfaces. Analysis of the data presented in Table 2 showed that the thickness of oxide films formed on the samples of tubes depended on the carbon content in the initial ingots (column 2). The higher is the carbon content in the metal of tubes, the greater is the thickness of the formed oxide films and the overweight. The effect of nitrogen and aluminum is weaker.

The results on ion irradiation and alloying of the surface by carbon shown in Table 2 and averaged thicknesses of the oxide film ( $\mu\text{m}$ ) on the outer surface of samples alloyed by carbon and combination of such elements as Mo-Fe-Al shown in Table 3 are new and interesting and their analysis makes it possible to point out the following features of the effect of ion modification of the surface layer on the corrosion resistance of fuel tubes.

Irradiation of the surface of alloys in the initial state by Ar<sup>+</sup> ions in the regime of ion sputtering for cleaning the surface (state I) results in a noticeable slowdown of the oxidation rate in comparison with oxidation of tubes in the initial state (compare columns 4 and 9 of Table 2). This conclusion follows from the analysis of the overweights and thicknesses of the oxide films.

Irradiation of the surface of alloys after chemical etching by Ar<sup>+</sup> ions in the regime of ion sputtering (state II) also improves the corrosion resistance of the alloys in spite of increasing the sputtered surface roughness parameter. Comparison of data presented in Table 2 (columns 4 and 9) shows that chemical etching and subsequent ion sputtering can significantly reduce the overweight and thickness of the film in comparison with the results of oxidation of the tube samples in the delivery state (column 9). Visual inspection and study of the structure of oxide films in depth shows that, in the first approximation, the oxide film structure is sufficiently uniform; the film has a classic dark color, but the “oxide-metal” interface copies the initial relief of the sputtered surface in the early

hours of oxidation (300 h). As a result, a wavy “metal-oxide” interface is formed, near of which pores 0.1-0.2  $\mu\text{m}$  in size are formed with increasing the oxidation time (fig. 2).

Implantation of carbon into the surface layer to a depth of 0.3  $\mu\text{m}$  at concentrations from 0.25 to 0.8 at% in the regime of ion mixing, as seen from the data in Table 2 (state III) and Table 3, results in slowdown of the corrosion at the oxidation time of 4320 h at low carbon concentrations of 0.35-0.50 at%. An abnormally high level of the overweight and thickness of the oxide on tube samples for smelting 5002 (Table 2) is probably due to increased pollution of the surface layer in the manufacture of tubes of this smelting, so that they require a special regime of ion mixing and alloying. However, this requires further study.

Implantation by ion mixing of the composition of Mo-Fe-Al elements into the surface layer to a depth of 0.7  $\mu\text{m}$  at concentrations from 0.15 to 0.25 at% of each element, as seen from Table 3, generally causes a noticeable decrease in the surface layer corrosivity, which is manifested in the reduction of the oxide film thicknesses (fig. 3). The film thicknesses considerably vary with increasing the oxidation time; for example, the film thickness is in the range of 0.5-1.4  $\mu\text{m}$  at 300 h of oxidation and it reaches 3-4  $\mu\text{m}$  at 4320 h of tests.

## Discussion of results

Results are obtained confirming the positive effect of ion irradiation on the corrosion behavior of alloy E110 with various content of impurity elements that have a negative influence on the corrosion resistance of the alloy, especially carbon [1, 7-9]. The action of ion irradiation in the regime of sputtering by  $\text{Ar}^+$  ions cleans in fact the surface layer from impurities and small defects and eliminates to a certain extent fine precipitates of the second phases. In fact, there is a certain modification of the structural-phase state of the surface layer. However, the accumulation of radiation defects in the treated layer under implantation of a part of  $\text{Ar}^+$  ions actually means increasing the free energy of the system and thus increasing the interaction of oxygen with zirconium, which results in active oxidation of zirconium in the first 300-720 h of oxidation. However, the advantage of this treatment is that a uniform film with good protective properties is formed and grows on the treated surface. Its advantages have an impact at large oxidation times.

In case of complex alloying of zirconium with elements in the form of a Mo-Fe-Al ternary composition, variation in the oxide film thickness is more complex. It was shown previously [3] that at high oxidation times increasing the thickness of oxide films on the initial surface, as shown in fig. 4a, changed according to a power law  $z = a_1 t^n$ , where  $n \leq 0.5$ . At that, the maximum growth rate of the oxide is observed on the samples of alloy E635, and the minimum one – on commercially pure zirconium.

Under oxidation of samples with an ion-alloyed surface (fig. 4b), the growth rate of films can be approximated by two linear areas. When the oxidation time is in the 10-600 h range, the oxide growth rate on all the samples is similar and a change of the thickness from the oxidation time is of the form  $z(\text{E100}) = A_1t+B_1$ ;  $z(\text{E110}) = A_2t+B_2$ ;  $z(\text{E635}) = A_3t+B_3$ ; and at the 1200-3000 h oxidation time, a change of the thickness decreases.

In general, the oxide film thickness for both the zirconium alloys has similar values (1.7 – 2.0  $\mu\text{m}$ ) at large oxidation times more than 3000 h. This suggests that under increasing the oxidation time of the ion-alloyed surface, the oxide film growth kinetics is determined by the alloying conditions and, to a lesser extent, depends on the composition of the initial alloy, the minimum increase of the film thickness occurring on the samples modified in the regime of a simultaneous complex (Mo-Fe-Al) alloying.

At least two processes occur during the implantation of Al, Fe and Mo atoms into the materials. First, ion bombardment and implantation of alloying atoms into the substrate result in accumulation of distortions of the crystal lattice and damages, i.e. an increase of the free energy level of atoms -  $\Delta G_{\text{chem}}$ . Second, significant internal (side) stresses are formed in a thin surface layer of the substrate because of implantation of Mo, Al and Fe atoms that are due to dilatation of the lattice by implanted atoms, which also leads to an excess of the free energy of atoms -  $\Delta G_{\text{elastic}}$ . The free energy excess ( $\Delta G = \Delta G_{\text{chem}} + \Delta G_{\text{elastic}}$ ) contributes to more active interaction of oxygen with atoms to form compounds, which decreases the level of the excess free energy of atoms.

Taking the modified surface uniformity into consideration, the corrosion front sufficiently uniformly advances deeper into the material. At that, the implanted atoms of Fe and Mo inhibit the advancement process of oxygen and the oxidation front deeper into the metal. A decrease of  $\Delta G$  and accumulation of shifted implanted atoms at the oxide formation front change the film growth kinetics (fig. 4b), i.e. inhibition of the oxide phase front growth, which decreases the oxidation rate of zirconium.

## Conclusion

The thickness of oxide films formed on the samples of tubes has been found to depend on the carbon content in the initial ingots and increasing the corrosion products with the carbon content in the alloys has been shown. The effect of nitrogen and aluminum is weaker.

Treatment of the samples after mechanical grinding and chemical polishing in the regime of sputtering by argon ions improves the surface state of samples, removing small defects, contaminants and particles of the second phases, which promotes the formation and growth of structurally uniform oxide films that do not have porosity and microcracks and have higher protective properties in comparison with films obtained on the untreated surface.

Implantation into the surface layer of a composition of such elements as Mo-Fe-Al to a depth up to 0.7  $\mu\text{m}$  with concentrations from 0.15 to 0.25 at% of each element in the regime of ion mixing causes a noticeable decrease of the surface layer corrosiveness, which is manifested in a significant reduction of the oxide film thickness.

## REFERENCES

1. Konkov V.F., Khokhunova T.N., Sablin M.N., Mileshkina O.Yu. «Obosnovaniye snizheniya verkhnego predela sodержaniya ugleroda v splave E110 po rezultatam korrozionnykh ispytany». Sbornik tezisov MAYaT-2012, p. 32.
2. Kalin B.A. Prospects for Radiation-Treatment Technologies for New Materials. - *IUMRS Facets*, 2002, Volume 2, No. 1, pp. 15-21.
3. Volkov N.V., Kalin B.A. Creating multilayer gradient surface layers with wide energy spectrum ion beams. Abstracts V Russian Chinese Workshop PPT-2009, 30.09-04.10 2009, Tomsk, RFBR, TPU, P.11.
4. Volkov N.V., Kalin B.A., Markelov V.A., Osipov V.V., Pimenov Yu.V. Investigation and Modification of the Structural-Phase State of Oxide Films on Zirconium Alloys. Proceedings of the 8<sup>th</sup> International Conference “WWER Fuel Performance, Modelling and Experimental Support” 26 September - 4 October 2009, Helena Resort, Bulgaria. Sofiya: Institute for Nuclear Research and Nuclear Energy. 2009. P463–471.
5. Kalin B.A., Volkov N.V. Ionny uskoritel VOKAL. V sb.: Materialovedcheskiye vorposy atomnoy tekhniki. M.: Energoatomizdat, 1991. pp. 64-67.
6. Komarov F.F. Ionnyaya implantatsiya v metally, M., 1984. 261 p.
7. Duglas D. Metallovedeniye tsirkoniya. M.: Atomizdat, 1975. 360 p.
8. Zaimovsky A.S., Nikulina A.V., Reshetnikov N.G. Tsirkoniyevye splavy v yadernoy energetike. M.: Energoatomizdat, 1994. 256 p.
9. Kalin B.A., Osipov V.V., Volkov N.V., Oleynikov I.V. Structure of Oxide Films on Ion-Modified Surface of Zirconium Alloys. – *Physics and Chemistry of Materials Processing*, 2004, №. 1, pp. 13-21.

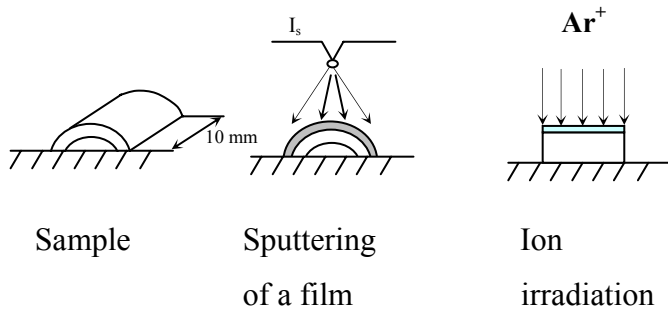


Fig. 1. A scheme of coating of a film onto the surface of a sample (using sputtering regime) and subsequent alloying by ion mixing under irradiation by  $\text{Ar}^+$  ions

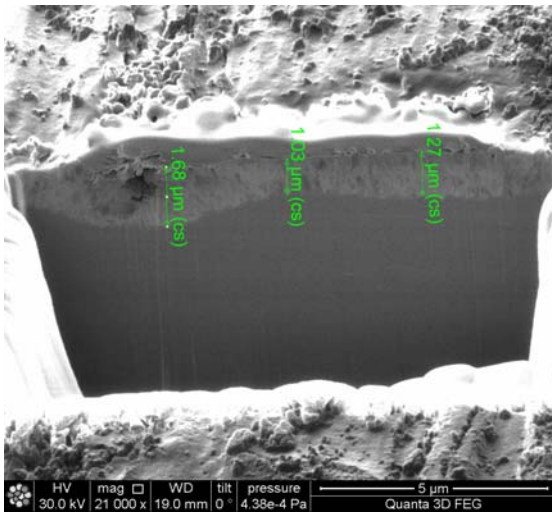


Fig. 2. Cross-section image of oxide films on a sample (smelting 5002) after oxidation for 300 h

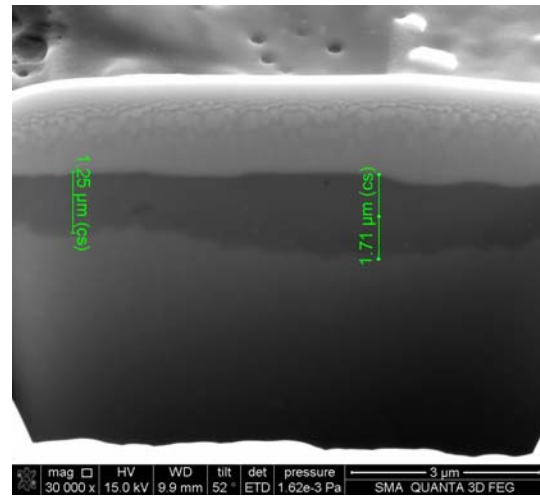
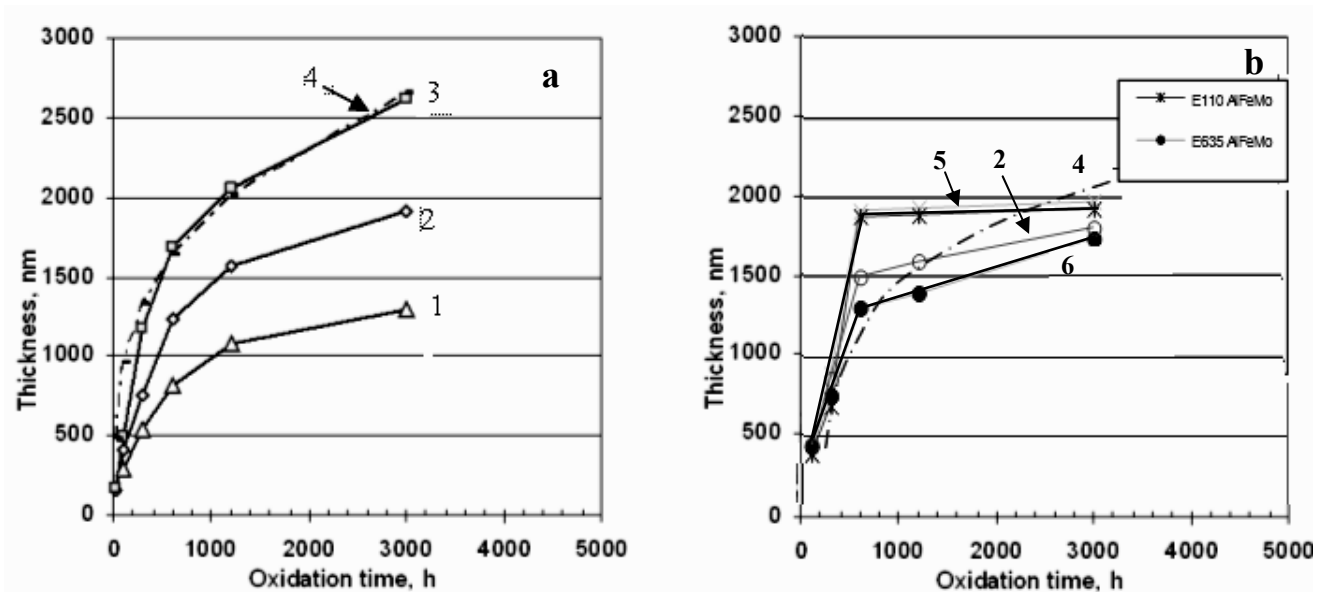


Fig. 3. Cross-section image of oxide films on a sample (smelting 5001/08) alloyed by the atoms of a Mo-Al-Fe three-layer film after oxidation for 300 h



1 – Zr100, 2 – E110, 3 – E635, 4 –  $z(t) = a t^{0.33} + \text{const}$ , 5 – E110 alloying by MoFeAl atoms, 6 – E635 alloying by MoFeAl atoms

Fig. 4. A change of the thickness of oxide films grown on the surface of zirconium and its alloys (data of overweights): a – in the initial state, b – after ion alloying (the dashed line shows the power law variation  $\sim t^{0.33}$ )

Table 1. Impurity composition of the investigated samples of tubes from alloy E110

Smelting number	Impurity composition, ppm		
	C	N	Al
5001 (Ø 9.5×8.33 mm)	140	41	58
5002 (Ø 9.5×8.33 mm)	120	37	58
5005 (Ø 9.10×7.93 mm)	79	35	63
5008 (Ø 9.10×7.93 mm)	98	40	80
5027 (Ø 9.10×7.93 mm)	100	39	50
301 (Ø 9.10×7.93 mm)	<100	<100	10

Table 3. Averaged thicknesses of the oxide film (µm) on the outer surface of the samples alloyed by carbon and a combination of elements Mo-Fe-Al

Smelting number	State of samples (layer of implantation)	Concentration of the implanted element by XRF analysis, at%	Test time, h		
			300	2160	4320
5002	Chem-Pol+Ar <sup>+</sup>	-	1.13±0.5	3.2±0.3	3.0±0.3*
	C (* 0.3 µm)	0.70	1.03- 1.68	-	3.3±0.3
	Mo-Fe-Al (* up to 0.7 µm)	0.25+0.20+0.30	-	-	2.0±0.3
5027	Chem-Pol +Ar <sup>+</sup>	-	1.2±0.5	1.7±0.3	3.7±0.3*
	C (0.3 µm)	0.50	0.67-1.17	-	3.3±0.3
	Mo-Fe-Al (* up to 0.7 µm)	0.35+0.20+0.20	-	1.5±0.3	3.0±0.3
5008	Chem-Pol +Ar <sup>+</sup>	-	0.8-1.1	-	2.9±0.3*
	C (0.3 µm)	0.37	-	-	2.0±0.3
	Mo-Fe-Al (* up to 0.7 µm)	-	-	-	2.0±0.3
5005	Chem-Pol +Ar <sup>+</sup>	-	1.24±0.5	1.7±0.3	2.5±0.3*
	C (0.3 µm)	0.25	0.43-0.92	-	2.9±0.3
	Mo-Fe-Al (* up to 0.7 µm)	-	-	-	2.1±0.3
301	Chem-Pol +Ar <sup>+</sup>	-	1.3±0.5	-	2.4±0.3*
	C (* 0.3 µm)	0.80	0.76±0.5	-	2.5±0.3
	Mo-Fe-Al (up to 0.7 µm)	-	-	-	2.0±0.3
5001-08	Chem-Pol +Ar <sup>+</sup>	-	1.0±0.5	-	2.3±0.3*
	C (* 0.3 µm)	0.55	0.32-1.04	-	2.7±0.3
	Mo-Fe-Al (* up to 0.7 µm)	0.20+0.20+0.15	-	1.5±0.3	2.1±0.3

\* – the implantation depth of elements

Table 2. State of the oxide films of tube samples from alloy E110 based on the sponge «Wah Chang» with a various treatment of the outer surface after autoclave tests in water at T = 360 °C and P = 18.6 MPa on the basis of 180 d

Smelt- ing number	Carbon content in the ingot, ppm	Type of treatment (state)	Over- weight/thickness of the oxide, mg/dm <sup>2</sup> / μm	Oxide thickness, μm			External view of the film	Overweight/thickness of the oxide in the ini- tial state on the basis of 3600 h, mg/dm <sup>2</sup> / μm
				SIM, outer	IR spec- tro- scopy, outer	IR spec- troscopy, internal		
1	2	3	4	5	6	7	8	9
5001	140	I	95.0 / 6.3	4.7±0.3	3.1±0.1	3.3±0.1	The film on the outer side has whitening areas.	151 / 10.0
		II	35.0 / 2.3	2.3±0.5	2.8±0.1	3.2±0.1	The film on the outer side is dark and uniform.	
		III	30.0 / 2.0	2.7±0.6	3.4±0.1	3.2±0.1	The film on the outer side is dark and uniform.	
5002	120	I	35.0 / 2.3	3.1±0.1	2.6±0.1	2.4±0.1	The film on the outer side has whitening areas.	135 / 8.9
		II	40.0 / 2.6	3.0±0.1	4.7±0.1	3.3±0.1	The film on the outer side is dark with the presence of whitening areas.	
		III	180.0 / 11.9	23.0±1.0	-	3.0±0.1	The film on the outer side is light and uniform; there are darkening areas.	
5005	79	I	30.0 / 2.0	3.0±0.5	2.6±0.1	2.5±0.1	The film is dark and uniform.	41 / 2.7
		II	45.0 / 3.0	3.4±0.4	2.9±0.1	3.3±0.1	The film on the outer side is dark; there are whitening areas.	
		III	30.0 / 2.0	2.9±0.2	2.6±0.1	2.6±0.1	The film on the outer side is dark.	
5008	98	I	40.0 / 2.6	3.8±0.1	2.3±0.1	2.4±0.1	The film on the outer side is dark.	43 / 2.9
		II	35.0 / 2.3	1.9±0.2	2.9±0.1	3.5±0.1	The film on the outer side is dark.	
		III	10.0 / 0.7	2.0±0.6	4.5±0.1	3.8±0.1	The film on the outer side is dark; there are whitening areas and shedding of faces.	
5027	97	Ir	200.0 / 13.2	10.5± 0.5	-	3.3±0.1	The film on the outer side is light; there are darkening areas.	36 / 2.4
		II	60.0 / 4.0	3.7±0.4	2.3±0.1	2.6±0.1	The film on the outer side is dark; there are whitening areas.	
		III	25.0 / 1.7	3.3±0.3	2.6±0.1	2.4±0.1	The film on the outer side is dark.	
301	<100	I	35.0 / 2.3	3.0±0.5	2.9±0.1	3.7±0.1	The film on the outer side is dark.	38 / 2.5
		II	45.0 / 3.0	2.4±0.3	3.4±0.1	3.8±0.1	The film on the outer side is dark and uniform.	
		III	45.0 / 3.0	2.5±0.2	3.3±0.1	3.9±0.1	The film on the outer side is dark; there are whitening areas.	